Available online at www.sciencedirect.com
ScienceDirect
Geochimica et Cosmochimica Acta 74 (2010) 2011–2024
Geochimica et Cosmochimica Acta
www.elsevier.com/locate/gca

Kinetic oxygen isotope effects during dissimilatory sulfate reduction: A combined theoretical and experimental approach

Alexandra V. Turchyn [a,*,1], Volker Brüchert [b], Timothy W. Lyons [c], Gregory S. Engel [d], Nurgul Balci [e], Daniel P. Schrag [f], Benjamin Brunner [g]

[a] Department of Earth and Planetary Science, University of California Berkeley, McCone Hall, Berkeley, CA, USA
[b] Department of Geology and Geochemistry, Stockholm University, Stockholm, Sweden
[c] Department of Earth Sciences, University of California, Riverside, CA, USA
[d] Department of Chemistry, University of Chicago, Chicago, IL, USA
[e] Department of Geological Engineering, Division of Ore Deposits and Geochemistry, Istanbul Technical University, Istanbul, Turkey
[f] Department of Earth and Planetary Sciences, Harvard University, Cambridge, MA, USA
[g] Max Planck Institute for Marine Microbiology, Bremen, Germany

Received 12 November 2008; accepted in revised form 4 January 2010; available online 14 January 2010

Abstract

Kinetic isotope effects related to the breaking of chemical bonds drive sulfur isotope fractionation during dissimilatory sulfate reduction (DSR), whereas oxygen isotope fractionation during DSR is dominated by exchange between intercellular sulfur intermediates and water. We use a simplified biochemical model for DSR to explore how a kinetic oxygen isotope effect may be expressed. We then explore these relationships in light of evolving sulfur and oxygen isotope compositions ($\delta^{34}S_{SO4}$ and $\delta^{18}O_{SO4}$) during batch culture growth of twelve strains of sulfate-reducing bacteria. Cultured under conditions to optimize growth and with identical $\delta^{18}O_{H2O}$ and initial $\delta^{18}O_{SO4}$, all strains show ^{34}S enrichment, whereas only six strains show significant ^{18}O enrichment. The remaining six show no (or minimal) change in $\delta^{18}O_{SO4}$ over the growth of the bacteria. We use these experimental and theoretical results to address three questions: (i) which sulfur intermediates exchange oxygen isotopes with water, (ii) what is the kinetic oxygen isotope effect related to the reduction of adenosine phosphosulfate (APS) to sulfite (SO_3^{2-}), (iii) does a kinetic oxygen isotope effect impact the apparent oxygen isotope equilibrium values? We conclude that oxygen isotope exchange between water and a sulfur intermediate likely occurs downstream of APS and that our data constrain the kinetic oxygen isotope fractionation for the reduction of APS to sulfite to be smaller than 4‰. This small oxygen isotope effect impacts the apparent oxygen isotope equilibrium as controlled by the extent to which APS reduction is rate-limiting.

1. INTRODUCTION

Dissimilatory sulfate reduction (DSR) and subsequent pyrite formation are two of the main fluxes in the marine biogeochemical sulfur cycle (Canfield, 2004). The sulfur and oxygen isotope compositions of sulfate ($\delta^{34}S_{SO4}$ and $\delta^{18}O_{SO4}$, respectively) have been the primary tools for exploring variability in the sulfur cycle, although much of the emphasis to date has been placed on $\delta^{34}S_{SO4}$ (e.g., Holser and Kaplan, 1966; Cameron, 1982; Canfield and Teske, 1996; Canfield, 1998; Paytan et al., 2004; Johnston et al., 2005; Wortmann and Chernyavsky, 2007). In organic-rich sediments, both $\delta^{34}S_{SO4}$ and $\delta^{18}O_{SO4}$ are affected by isotope fractionations during microbially mediated processes and,

* Corresponding author. Tel.: +44 1223 333479.
E-mail addresses: atur07@esc.cam.ac.uk, avt25@cam.ac.uk (A.V. Turchyn).
[1] Present address: University of Cambridge, Department of Earth Sciences, Downing Street, Cambridge, United Kingdom.

0016-7037/$ - see front matter © 2010 Elsevier Ltd. All rights reserved.
doi:10.1016/j.gca.2010.01.004

in the case of $\delta^{18}O_{SO4,}$ varying degrees of equilibration with water (e.g., Mizutani and Rafter, 1973; Fritz et al., 1989; Böttcher et al., 1998, 1999; Brunner et al., 2005; Böttcher et al., 2005; Wortmann et al., 2007). Constraining what controls the magnitude of these isotope fractionations for sulfur and oxygen isotopes and understanding the relationship between the two isotope systems remains critical for rigorous interpretation of both local and global temporal variability.

Controls on the magnitudes and pathways of the sulfur isotope fractionation during DSR (ε_S) are far better understood than those for oxygen (ε_O). ε_S ranges between 2 and 46‰ or even higher (Rudnicki et al., 2001; Wortmann et al., 2001); theoretical studies have suggested that its magnitude is a function of various physiological and environmental constraints (Rees, 1973; Canfield, 2001b; Brüchert, 2004; Brunner and Bernasconi, 2005; Brunner et al., 2005). Further experimental studies have confirmed the importance of diverse factors on the magnitude of ε_S, such as specific microbial metabolisms and carbon sources (Kaplan and Rittenberg, 1964; Detmers et al., 2001; Brüchert, 2004), rate of sulfate reduction (Habicht and Canfield, 2001), amount of sulfate available (Canfield, 2001a; Habicht et al., 2002), and temperature (Brüchert et al., 2001; Canfield et al., 2006). Our understanding of ε_S and specifically the controls underlying its variable magnitude have allowed us to explore diverse themes ranging from microbial processes in modern organic-rich sediments and corresponding oxidation of organic matter on the local scale (Jørgensen, 1979, 1990) to the behavior of the sulfur cycle on early Earth (e.g., Habicht et al., 2002; Kah et al., 2004; Johnston et al., 2005). The additional use of oxygen isotopes in sulfate to explore microbial redox processes and possibly to reconstruct variability in the marine sulfur cycle over Earth history has shown promise (e.g., Turchyn and Schrag, 2006). The added strength of this coupled sulfur and oxygen isotope approach will only grow with an improved understanding of the controls on oxygen isotope fractionation during DSR.

1.1. Open questions about ε_O and the S–O relationship in sulfate

Sulfate ions do not exchange their oxygen atoms with water readily at the temperature and pH of most natural environments, at least not on timescales equivalent to the lifetime of a sulfate molecule ($\sim 10^6$ years: Lloyd, 1968; Zak et al., 1980). However, many studies have demonstrated that the oxygen isotope composition of sulfate during DSR is influenced by the isotopic composition of water in which the bacteria are grown (e.g., Mizutani and Rafter, 1973; Fritz et al., 1989; Brunner et al., 2005; Mangalo et al., 2007; Farquhar et al., 2008). The conclusion has been that oxygen isotope exchange between sulfur compounds and water occurs within the cell, likely when the sulfur is in an intermediate state such as adenosine phososulfate (APS) (Kemp and Thode, 1968; Mizutani and Rafter, 1973) or sulfite (Fritz et al., 1989). Further, water oxygen is incorporated during the oxidation of these sulfur intermediates back to sulfate, and particularly the oxidation of sulfite to APS via adenosine monophosphate (AMP) has been invoked as a potentially important mechanism for water–oxygen incorporation (Peck and Stulberg, 1962; Fritz et al., 2002; Wortmann et al., 2007). The incorporation of oxygen from water into sulfate during DSR has been observed in various settings, including deep-sea pore-fluid profiles (Böttcher et al., 1998, 1999; Wortmann et al., 2007) and sediment incubation experiments (Fritz et al., 1989; Böttcher et al., 2001; Brunner et al., 2005; Farquhar et al., 2008).

Several aspects of oxygen isotope fractionation during DSR, however, remain unresolved; here we highlight four outstanding questions concerning the mechanism of oxygen isotope fractionation during DSR. A first major issue is that we have yet to identify the precise sulfur compounds that exchange oxygen with water during the stepwise reduction of sulfate to sulfide. While the likely intermediate compounds were listed above, it is unclear which of these dominates or whether it is primarily during the reoxidation of these compounds to sulfate that the water–oxygen is incorporated (Fritz et al., 1989; Wortmann et al., 2007).

A second issue is that, similar to sulfur isotopes, kinetic oxygen isotope effects should occur during the enzymatically driven steps of DSR (e.g., Mizutani and Rafter, 1973; Grinenko and Ustinov, 1990). The magnitude of kinetic oxygen isotope fractionation associated with the various enzymes has not been assessed, and it is unknown whether these fractionations contribute to the observed behavior of oxygen in sulfate or if these effects are fully overprinted by oxygen exchange between sulfur intermediates and water. Several studies observing persistently coupled $\delta^{34}S_{SO4}$ and $\delta^{18}O_{SO4}$ behavior during DSR have suggested that in certain environments kinetic isotope effects could be important; these settings span sulfidic waters (Mandernack et al., 2003), seeps in the Gulf of Mexico (Aharon and Fu, 2000), organic-rich sediments in the Cascadia margin (Bottrell et al., 2000), lake samples from New Zealand (Mizutani and Ragter, 1969), and pure-culture growth experiments (Grinenko and Ustinov, 1990).

A third outstanding issue for oxygen isotope behavior during DSR is that there is a range of apparent equilibrium oxygen isotope fractionation observed between sulfate and water in both laboratory experiments and natural environments. Like any equilibrium isotope fractionation, the equilibration of oxygen isotopes between sulfate or sulfur intermediates and water is temperature dependent; the higher the temperature the lower the fractionation. In a pioneering study, Fritz et al. (1989) observed that the equilibrium oxygen isotope fractionation was 25‰ at 30 °C, increasing to 29‰ at 5 °C. Consistent with these results, laboratory experiments performed at 27 °C suggested fully equilibrated oxygen isotope fractionation at 24‰ and 26‰ (Böttcher et al., 1998, 1999, respectively). Measurements made in deep-sea sediments at colder temperatures, however, suggested apparent equilibrium oxygen isotope fractionation of 27.93‰ (corrected for temperature based on the pore fluid data from Wortmann et al. (2007)), while equilibrium values of 38.4‰ were derived from measurements in 0 °C glacial beds (Wadham et al., 2004). All these observed values differ from the equilibrium value predicted for pure sulfate–water oxygen isotope exchange from high temperature experiments (36.4‰, Lloyd, 1968 and 33.6‰, Mizutani and Rafter, 1973). Some of this range could re-

flect changes in the $\delta^{18}O_{SO4}$ during DSR misinterpreted as full equilibrium exchange values when true isotope equilibrium had not been attained (as suggested in Wortmann et al., 2007), or kinetic oxygen isotope effects that are overprinted by equilibrium exchange with water to varying degrees (as suggested in Mizutani and Rafter, 1973). Alternatively, the range could represent other environmental or physiological factors in addition to temperature that impact the expressed equilibrium oxygen isotope fractionation between sulfur compounds and water.

A fourth and final observation of oxygen isotopes during DSR is that large sulfur isotope effects coincide with increased oxygen isotope exchange between water and sulfur compounds (Mizutani and Rafter, 1973; Basharmal, 1985; Van Stempvoort and Krouse, 1994; Mangalo et al., 2007). Since the magnitude of sulfur isotope fractionation depends on both the enzymatic kinetic isotope fractionation and the ratio of forward and backward fluxes of sulfur intermediates within the cell, it follows that increased sulfur isotope fractionation would result in increased expression of oxygen isotope exchange in the extracellular sulfate pool (Mangalo et al., 2007; Wortmann et al., 2007). Despite this past work, the precise mechanistic relationship between sulfur and oxygen isotope fractionation during DSR remains insufficiently explored.

In this paper we begin with the assumption that a kinetic oxygen isotope effect should occur during the various steps during DSR and, from a theoretical viewpoint, assess how this effect may be expressed. Using a modified version of a DSR biochemical model for the flow of sulfur through the bacterial cell during DSR, we explore the consequences of this kinetic oxygen isotope fractionation – combined with possible oxygen isotope exchange – on patterns of sulfur and oxygen isotope fractionation during DSR. We compare the model results with oxygen and sulfur isotope data from batch culture growth experiments for twelve strains of sulfate-reducing bacteria to elucidate the relative importance of kinetic vs. equilibrium oxygen isotope effects during DSR.

2. A MODIFIED MODEL FOR SULFUR AND OXYGEN ISOTOPES

To better understand the potential impact of a kinetic oxygen isotope effect during sulfate reduction, we use a biochemical model for DSR wherein both equilibrium and kinetic oxygen isotope effects are included (see schematic Fig. 1). Rees (1973) first developed this type of model – exploring the various enzymatic steps during DSR and the related sulfur isotope fractionations. This model has been modified over the years to include various sites of oxygen isotope fractionation and exchange within the reaction network (Fritz et al., 1989; Farquhar et al., 2003; Brunner and Bernasconi, 2005; including the possibility of exchange via AMP – Wortmann et al., 2007). Acknowledging the foundation provided by Rees (1973), we refer to our model as a "modified Rees (1973) model". Because this model has been presented in detail elsewhere (Brunner et al., 2005; Wortmann et al., 2007) we emphasize only those aspects most relevant to our work.

The major biochemical steps during DSR are incorporation of sulfate into the cell, activation to APS, reduction of APS to sulfite, and reduction of sulfite to hydrogen sulfide (Fig. 1) and all these enzymatic steps are reversible. Net sulfur isotope fractionation (ε_S) is controlled by kinetic isotope effects during both the reduction of APS to sulfite ($\varepsilon^{34}S_{APS-SO3} = 25‰$) and the reduction of sulfite to sulfide ($\varepsilon^{34}S_{SO3-H2S} = 25‰$ to 50‰), and by the ratio of the forward and backward fluxes of all the biochemical steps (see Brunner and Bernasconi, 2005 for discussion). Sulfur isotope fractionations larger than 25‰ are only seen in the extracellular sulfate pool if $\varepsilon^{34}S_{SO3-H2S}$ is expressed – that is, APS reduction to sulfite is not rate-limiting.

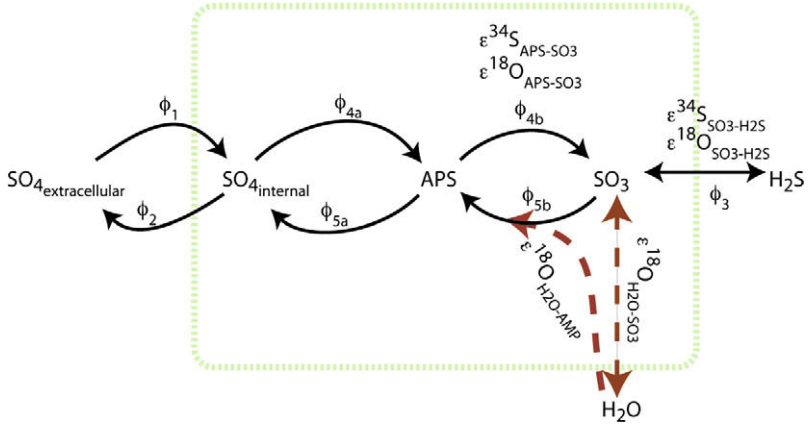

Fig. 1. Schematic model for oxygen and sulfur isotope effects. Sulfur isotope effects are controlled by the enzymatic kinetic sulfur isotope effects for the various steps (APS to sulfite and sulfite to sulfide) as well as by the ratio between the forward and backward fluxes. Oxygen isotope effects are also controlled by the enzymatic kinetic oxygen isotope effects for APS reduction to sulfite and sulfite reduction to sulfide. However, the oxygen isotope effect related to the reduction of sulfite to sulfide is overprinted by oxygen isotope exchange between water and sulfite and reoxidation of sulfite to APS with oxygen derived from adenosine monophosphate (AMP). Therefore, in the discussion, we do not address oxygen isotope effects related to the reduction of sulfite to sulfide. The oxygen isotope effect related to the reduction of APS to SO_3 can be expressed as: $\varepsilon^{18}O_{APS-SO3} = k \times \varepsilon^{34}S_{APS-SO3}$. This biochemical model for sulfate reduction including oxygen isotope fractionation was first introduced by Fritz et al. (1989) and further modified by Brunner et al. (2005) and Wortmann et al. (2007).

For oxygen isotope fractionation during DSR, we assign a kinetic oxygen isotope effect to the reduction of APS to sulfite ($\varepsilon^{18}O_{APS-SO3}$) at ¼ the sulfur isotope effect ($\varepsilon^{34}S_{APS-SO3}$), a ratio that was suggested by previous environmental studies (e.g., Grinenko and Ustinov, 1990; Mandernack et al., 2003). We can vary this number considerably to probe the effect of a kinetic oxygen isotope effect on the evolution of the $\delta^{18}O_{SO4}$. In addition, an equilibrium oxygen isotope fractionation between intermediate sulfur species and water is assigned. Two species have been proposed to equilibrate oxygen isotopes with ambient water: APS and sulfite. Recent work has suggested that oxygen isotope exchange between APS and water is unlikely (Kohl and Bao, 2006), whereas oxygen isotope exchange between sulfite and water has been observed in abiotic experiments (e.g., Betts and Voss, 1970; Horner and Connick, 2003, and references therein). The magnitude of equilibrium oxygen isotope fractionation between sulfite and water, and the controls on its variability, remain somewhat unresolved; recent experiments suggest the equilibrium sulfite–water fractionation is larger than 14‰ and likely smaller than 28‰ (Brunner et al., 2006). The second mechanism for water–oxygen incorporation into the sulfate molecule in our model is from ambient water or oxygen in AMP during the reoxidation of sulfite (Wortmann et al., 2007). As long as the reduction of APS to sulfite is reversible (i.e., APS reduction is not rate-limiting), the proposed oxygen isotope exchange between sulfite and water and subsequent oxidation of sulfite to APS will be the dominant processes for incorporating water–oxygen into extracellular sulfate.

The expression of isotope fractionation in the extracellular sulfur pool depends on the ratio of intracellular forward and backward fluxes (i.e., the relative reversibility of the various steps during DSR — Fig. 1) and requires the ability of isotopically modified sulfate (or APS) to pass across the membrane into the extracellular pool. Specifically, the reversibility of the reduction of APS to sulfite (ϕ_{4b}/ϕ_{5b}) plays a key role in the expression of sulfur and oxygen isotope fractionation during DSR. If APS reduction is rate-limiting (and therefore not reversible, $\phi_{5b} = 0$), neither sulfur isotope effects related to the reduction of sulfite to sulfide nor oxygen isotope exchange between sulfite and water (or sulfite–AMP) will be expressed. In this case, only a kinetic isotope effect associated with APS reduction to sulfite ($\varepsilon^{34}S_{APS-SO3}$ and $\varepsilon^{18}O_{APS-SO3}$) will be seen. Thus, in a plot of $\delta^{18}O_{SO4}$ vs. $\delta^{34}S_{SO4}$ during DSR, only a single linear relationship is possible (trend A in Fig. 2). It therefore holds that:

$$\varepsilon_O = k \times \varepsilon_S, \quad (1)$$

here ε_O and ε_S are the oxygen and sulfur kinetic isotope effects assuming Rayleigh-style distillation in a closed system and the slope (k) should be constant among sulfate-reducing bacteria. Because APS reduction in this scenario is rate-limiting, the ratio between ε_O and ε_S is equivalent to the ratio between $\varepsilon^{18}O_{APS-SO3}$ and $\varepsilon^{34}S_{APS-SO3}$ in Fig. 1. There are two major consequences that follow. First, when APS reduction is rate-limiting, there is no limit to the oxygen and sulfur isotope enrichment as DSR progresses (Fig. 2). Second, plots of $\delta^{18}O_{SO4}$ vs. $\delta^{34}S_{SO4}$ during DSR growth experiments with different sulfate-reducing bacteria should yield the same slope (k) (e.g., Brunner et al., 2005).

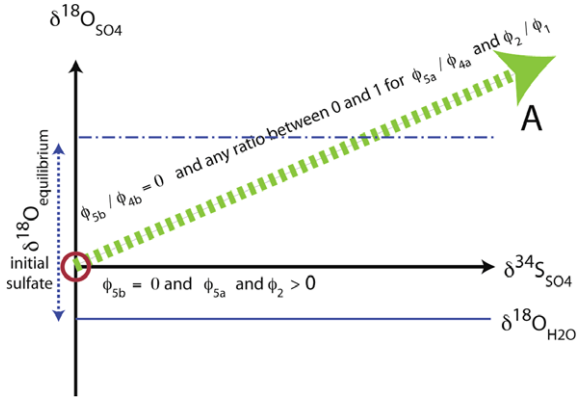

Fig. 2. The effect of kinetic isotope fractionation on sulfur–oxygen relationship during DSR. Both sulfur isotope and oxygen isotope effects are controlled by the kinetic isotope fractionation related to the reduction of APS to sulfite and by the ratio between forward and backward fluxes. Since the ratio between the kinetic sulfur and oxygen isotope effects is constant, and the ratio of the various fluxes impacts sulfur and oxygen isotope fractionation in the same way, only one O–S relationship is observed (trend A). See text for details.

It is likely, however, that in many cases APS reduction is not rate-limiting and is reversible ($\phi_{5b} \neq 0$). This makes the situation more complicated: kinetic sulfur and oxygen isotope effects during APS reduction, oxygen isotope exchange between sulfite and water or AMP and water, and kinetic sulfur and oxygen isotope effects related to the reduction of sulfite to sulfide will all be variably expressed in the extracellular sulfate pool. A consequence of APS reversibility during DSR is that there will be a limit in the magnitude of the oxygen isotope enrichment in the extracellular sulfate pool with progressive DSR. To describe the $\delta^{18}O_{SO4}$ limit we use the term 'apparent oxygen isotope equilibrium' – $\delta^{18}O_{apparent\ equilibrium}$ – which was first coined by Wortmann et al. (2007) to highlight that this value is not the true isotope equilibrium value ($\varepsilon^{18}O_{exchange}$). The $\delta^{18}O_{apparent\ equilibrium}$ is calculated as follows (see Appendix A for details):

$$\delta^{18}O_{apparent\ equilibrium} = \delta^{18}O_{water} + \varepsilon^{18}O_{exchange} + (\phi_{4b}/\phi_{5b}) \times \varepsilon^{18}O_{APS-SO3}, \quad (2)$$

where $\delta^{18}O_{water}$ is the oxygen isotope composition of the water, $\varepsilon^{18}O_{exchange}$ is the equilibrium oxygen isotope exchange (assumed to be between sulfite and water in our model) and $\varepsilon^{18}O_{APS-SO3}$ is the kinetic oxygen isotope effect associated with APS reduction.

As Eq. (2) demonstrates, the $\delta^{18}O_{apparent\ equilibrium}$ will depend on the reversibility of the reduction of APS to sulfite (ϕ_{4b}/ϕ_{5b}). If this step is fully reversible ($\phi_{4b}/\phi_{5b} = 1$), the influence of any kinetic oxygen isotope effect is minimized and the extracellular $\delta^{18}O_{SO4}$ will reach $\delta^{18}O_{apparent\ equilibrium}$ rapidly during DSR as shown in Fig. 3 as trend C. The $\delta_{18}O_{apparent\ equilibrium}$ in this case will be equal to the $\delta^{18}O_{water} + \varepsilon^{18}O_{exchange} + \varepsilon^{18}O_{APS-SO3}$, where the final two terms have a potential temperature dependence. If reduction of APS to sulfite is not fully reversible ($\phi_{4b}/\phi_{5b} > 1$), kinetic oxygen isotope effects can become more important. This is because reduced reversibility of the APS reduction step

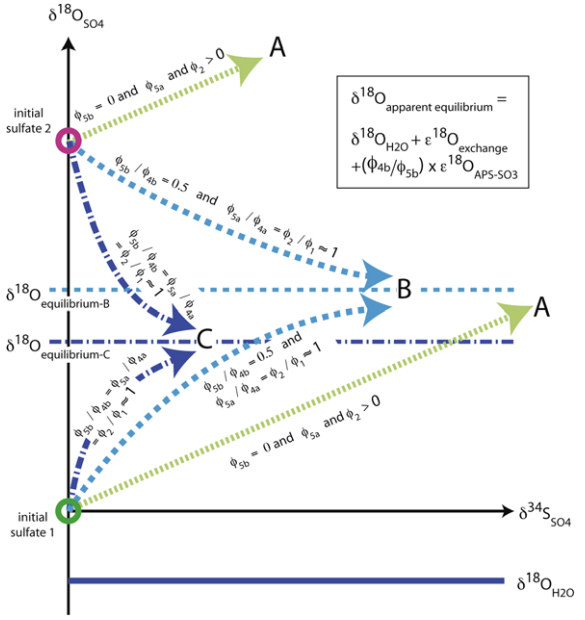

Fig. 3. Combination of kinetic oxygen isotope fractionation and oxygen isotope exchange. The sulfur–oxygen isotope relationship depends on the oxygen isotope composition of water and initial sulfate, and on the reversibility of the reduction of APS to sulfite. If the oxygen isotope composition of sulfate is below the apparent oxygen isotope equilibrium for fully reversible APS reduction ($\delta^{18}O_{equilibrium\text{-}C}$), oxygen isotope enrichment is observed in all cases (trends A, B, and C for initial sulfate 1). Positive and negative correlation between O and S isotopes is observed when the oxygen isotope composition of initial sulfate is higher than the apparent oxygen isotope equilibrium for fully reversible APS reduction (trend A, B, and C for initial sulfate 2). See text for details.

partially suppresses the expression of oxygen isotope exchange downstream of APS but does not affect the kinetic oxygen isotope fractionation related to the reduction of APS to sulfite. In this case, $\delta^{18}O_{apparent\ equilibrium}$ is reached more slowly and, importantly for this study, the value of $\delta^{18}O_{apparent\ equilibrium}$ is higher (trend B in Fig. 3). Ultimately, as APS reduction becomes rate-limiting, the slope of trend B in Fig. 3 will approach trend A in Figs. 2 and 3.

To summarize, if we plot $\delta^{18}O_{SO4}$ vs. $\delta^{34}S_{SO4}$ during DSR, our modified Rees (1973) model suggests the following:

- If APS reduction to sulfite is rate-limiting ($\phi_{5b} = 0$), sulfur and oxygen isotopes should exhibit a constant linear relationship that reflects the ratio between the kinetic isotope effect for sulfur and oxygen during APS reduction and should be constant among sulfate-reducing bacteria (Fig. 2).
- DSR experiments that yield even small differences in slopes in a plot of $\delta^{18}O_{SO4}$ vs. $\delta^{34}S_{SO4}$ are evidence for sulfite reoxidation and incorporation of oxygen from water into sulfur compounds.
- If APS reduction to sulfite is fully reversible ($\phi_{4b}/\phi_{5b} = 1$), the extracellular $\delta^{18}O_{SO4}$ will rapidly reach the apparent oxygen isotope equilibrium; whereas if reduction of APS to sulfite is not fully reversible ($\phi_{4b}/\phi_{5b} > 1$), the apparent oxygen isotope equilibrium is reached more slowly, but with higher $\delta^{18}O_{apparent\ equilibrium}$. This relationship is because reduced reversibility of this APS reduction step partially suppresses the expression of oxygen isotope exchange downstream of APS but does not affect the kinetic oxygen isotope fractionation related to the reduction of APS to sulfite.
- The $\delta^{18}O_{apparent\ equilibrium}$ should be affected by the kinetic oxygen isotope effect during APS reduction by varying amounts depending on the overall reversibility of APS reduction (ϕ_{4b}/ϕ_{5b} – Fig. 3).

These predictions provide a framework for the interpretation of our experimental results.

3. ANALYTICAL METHODS

DSR experiments were carried out with twelve different strains under optimal growth conditions in nutrient-replete culture medium. Details regarding the growth conditions, sampling methods, $\delta^{34}S_{SO4}$ data, and the corresponding sulfate concentrations were published previously (Detmers et al., 2001). We describe here only the analytical methods that concern the new oxygen isotope measurements. Prior to precipitating barium sulfate ($BaSO_4$) from the culture media, trace-metal grade acid was added to lower the pH to 4 to prevent precipitation of barium carbonate. Exposure to acid was too short (~2 h) to cause oxygen isotope exchange between sulfate and water (Lloyd, 1968). A 0.5 M barium chloride solution was then added to precipitate $BaSO_4$. The precipitate was washed briefly with deionized water and dried. The precipitated $BaSO_4$ was archived and later analyzed for its oxygen isotope composition at Harvard University's Laboratory for Geochemical Oceanography. Between 400 and 600 μg of $BaSO_4$ were weighed into silver capsules, dried thoroughly, and crushed with 1 mg of platinum powder. The samples were then pyrolyzed at 1450 °C in a Temperature Conversion Element Analyzer (TC/EA), and the resulting carbon monoxide (CO) was measured by continuous flow on a Delta Plus mass spectrometer. We made four measurements for each sample; the average and standard deviation of these replicate analyses are presented. NBS-127, a $BaSO_4$ standard, was run in replicate before and after every sample to correct for drift and to check for measurement error in the mass spectrometer. Samples were corrected to the $\delta^{18}O$ value of NBS-127 (9.3‰). Analytical precision based on numerous replicate measurements of NBS-127 was ±0.4‰ (2σ), but the standard deviations presented in our results are from the individual measurements of each sample. An additional laboratory-made standard was run in replicate with the NBS-127 sample (value 18‰ ± 0.6‰) as a cross check for analytical drift and machine precision. All oxygen isotope values determined are bracketed by the $\delta^{18}O_{SO4}$ of the two standards.

To further explore the relative importance of kinetic vs. oxygen isotope effects, we use the $\delta^{18}O_{SO4}$ and $\delta^{34}S_{SO4}$ of the evolving sulfate pool and the calculated fraction of sulfate remaining to determine the kinetic sulfur (ε_S) and oxygen (ε_O) isotope fractionation and the oxygen isotope exchange parameter (θ_O) based on linear regressions. The

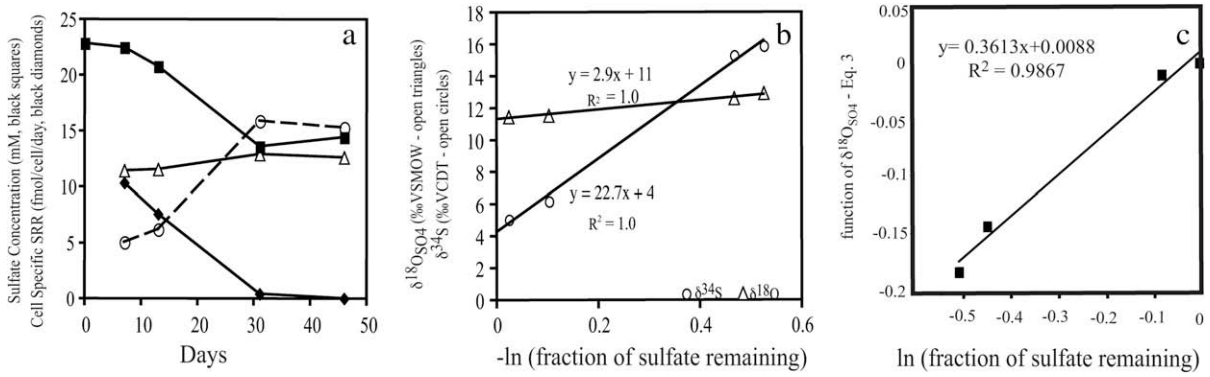

Fig. 4. Sample calculation for *Desulfofrigus oceanense*. (a) Sulfate concentrations (mM, black squares), $\delta^{34}S$ and $\delta^{18}O$ sulfate (‰ vs. VCDT/open circles and VSMOW/open triangles, respectively), and cell-specific sulfate reduction rates (mol/cell/day, black diamonds) determined by short-term (4 h) incubations at each time point (Brüchert et al., 2001; Detmers et al., 2001). (b) Rayleigh plots of $\delta^{34}S_{SO4}$ (in units ‰ CDT in open circles) and $\delta^{18}O_{SO4}$ (in units ‰VSMOW in open triangles) vs. the negative logarithm of the fraction of sulfate remaining at each time point. The lines represent linear regressions through the data and the slope is the respective isotope fractionation. (c) Plot for the determination of the parameter θ_O (Eq. (3)). The line represents the linear regressions through the data and the slope is the value of θ_O.

Table 1
Full data table for growth of sulfate-reducing bacteria and time evolution of sulfate concentrations and sulfur and oxygen isotope measurements.

Species name	Days	SO_4[a]	$\delta^{34}S$[a]	$\delta^{18}O$[b]	Stdev[b]	Species name	Days	SO_4[a]	$\delta^{34}S$[a]	$\delta^{18}O$[b]	Stdev[b]
Desulfococcus niacini	0	25.6	−1.4	13.76	0.09	*Desulfonatronovibrio*	0	26.9	2.8	13.29	0.30
	5	24.4	−1.1	13.58	0.21	*hydrogenovorans*	5	21.8	4.1	13.32	0.34
	7	25.3	−0.7	13.98	0.32		8	16.9	5.5	12.87	0.04
	11	24.0	−04	13.87	0.07		10	16.6	9.3	13.48	0.36
	48	16.2	2.5	14.49	0.06		13	17.2	6.1	12.56	0.12
Desulfonema magnum	0	26.9	−1.2	13.87	0.43	*DesulfiKella halophila*	0	15.9	2.7	12.13	0.20
		24.5	−0.9	13.10	0.28		5	9.2	11.1	14.00	0.23
	7	25.3	0.3	12.81	0.17		8	9.9	11.6	15.90	0.18
	11	23.1	0.8	13.72	0.36		10	9.8	11.7	17.29	0.71
	4S	19.1	9.6	14.26	0.38		13	11.0	11.3	16.78	0.32
Desulfovibrio profundus	0	20.7	3.6	13.9	0.38	*Desulfobulbus marinus*	0	19.2	3.0	12.54	0.38
	3	21.1	4.1	13.66	0.55		2	20.3	4.6	12.79	0.32
	5	12.4	5.2	13.73	0.61		9	6.3	21.7	15.86	0.07
	8	15.1	6.9	13.69	0.26		14	6.1	21.6	15.76	0.24
Desulfobacca acetooxidans	0	27.0	−1.3	13.14	1.03	*Desulfobulbus elongatus*	0	21.1	1.0	12.29	0.28
	7	20.5	0.7	14.14	0.91		3	21.5	2.3	12.54	0.54
	11	20.4	3.9	13.67	0.17		10	8.3	19.2	13.89	0.21
	18	8.1	18.6	16.73	0.38		12	8.1	19.7	14.93	0.18
	22	7.0	28.4	18.30	0.22		15	18.8	19.5	14.90	0.69
Desulfotomaculum	0	20.5	3.0	12.7	0.51	*Desulfosarcina variabilis*	0	21. 6	3.4	12.44	0.10
geothermicum	4	23.6	3.1	13.45	0.45		5	21.5	6.6	14.00	0.32
	6	16. 4	11.1	14.37	0.77		8	18.3	13.2	14.85	0.24
	7	15.5	11.4	14.06	0.82		10	15.5	16.3	15.39	0.14
	10	15.0	11.6	13.48	0.74		13	16.9	17.5	15.90	0. 29
Desulfobacterium	0	26.1	−2.34	12.84	0.91	*Desulfofrigus oceanense*	7	22.5	5.1	11.46	0.09
autotrophicum	1	28.7	−2.12	n/a	n/a		13	20.8	6.2	11.55	0.45
	4	26.5	−1.22	12.77	0.30		31	13.6	15.9	12.93	0.24
	5	25.3	−1.14	13.24	0.08		46	14.4	15.3	12.63	0.14
	6	25.9	−0.63	13.01	0.42						
	11	22.7	1.32	12.25	0.24						

[a] From Detmers et al. (2001), except *Desulfofrigus oceanense*, which is from Brüchert et al. (2001).
[b] Oxygen isotope in sulfate are an average of four replicate measurements and the 2_σ standard deviation is based on the replicate measurements.

calculation of ε_O and ε_S is only applicable to kinetic isotope fractionation since it is built on the assumption of closed-system behavior as modeled by a Rayleigh distillation; the parameter θ_O allows us to assess oxygen isotope exchange (Brunner et al., 2005). θ_O is a measure of the ratio between apparent oxygen isotope exchange and sulfate reduction rate;

$$\ln\left(\frac{\delta^{18}O_{SO4}(t)-(\delta^{18}O_{H2O}+\varepsilon^{18}O_{H2O\text{-}SO4})}{\delta^{18}O_{SO4}(t_0)-(\delta^{18}O_{H2O}+\varepsilon^{18}O_{H2O\text{-}SO4})}\right) = \theta_O \times \ln\left(\frac{SO_4(t)}{SO_4(t_0)}\right), \quad (3)$$

where $\delta^{18}O_{SO4}(t)$ is the oxygen isotope composition of sulfate at time t, $\delta^{18}O_{SO4}(t_0)$ the initial oxygen isotope composition of sulfate, $\delta^{18}O_{H2O}$ the oxygen isotope composition of water (−7.5‰ determined during experiments performed in the same lab at the same time and constant for all strain growths – Böttcher et al., 2001), $\varepsilon^{18}O_{H2O\text{-}SO4}$ is the equilibrium oxygen isotope fractionation between water and sulfate at a given temperature (+28.3‰ at 25 °C – derived from Mitzutani and Rafter, 1969; Mizutani, 1972; McKenzie and Truesdell, 1977; Fritz et al., 1989), $SO_4(t)$ is the amount of sulfate at time t, and $SO_4(t_0)$ the initial amount of sulfate. Strictly speaking, neither ε_O nor θ_O are relevant to combined kinetic and equilibrium oxygen isotope effects, because ε_O is calculated on the assumption of pure kinetic isotope fractionation, while θ_O is calculated on the assumption of pure oxygen isotope exchange in absence of kinetic isotope effects. A representative example of our calculations is shown in Fig. 4 for *Desulfofrigus oceanense*, with the graphical basis for the calculation of ε_S and ε_O shown in Fig. 4b and the calculation of θ_O shown in Fig. 4c.

4. ANALYTICAL RESULTS

The time evolution of sulfate concentration, $\delta^{34}S_{SO4}$, and $\delta^{18}O_{SO4}$ over the course of the growth experiments are presented in Table 1. The reported $\delta^{18}O_{SO4}$ data are the average of four replicate measurements, with the 2σ standard deviation listed for each measurement. The $\delta^{18}O_{SO4}$ of the initial sulfate was the same in all experiments (13.22‰ ± 0.28‰, $n = 12$) as was the $\delta^{18}O$ of the water. The average standard deviation over all measurements was 0.33‰, which compares well with the average precision of replicate measurements for the standard NBS-127 (±0.4‰). The errors for the sulfur isotope measurements were reported in Detmers et al. (2001; 0.3‰ based on replicate measurements of a laboratory standard). Table 2 provides a summary of the calculated isotope fractionation parameters (ε_S, ε_O, and θ_O), as well as cell-specific sulfate reduction rates, preferred marine habitat, and complete- vs. incomplete-oxidizing carbon metabolism. There are slight differences in the calculated ε_S from the original Detmers et al. (2001) publication because we used a linear rather than non-linear regression (because of the better fit with the oxygen isotope data). The calculated isotope enrichment factors are between 6.2‰ and 28.6‰ for sulfur (ε_S) and between −2.3 and 6.1‰ for oxygen (ε_O). The values calculated for the parameter θ_O are between −0.29 and 0.86.

Table 2
Calculated sulfur isotope kinetic fractionation factors (ε_S), oxygen isotope kinetic fractionation factors (ε_O), and oxygen isotope exchange parameter (θ_O) for all twelve species, including the 1σ standard deviation on the calculated fractionations. Further to the right in the table the habitat, temperature of the experiment, calculated oxygen isotope equilibrium fractionation factor between sulfite and water at that temperature (see text for references), bacterial metabolism (incomplete- vs. complete-oxidizing), calculated sulfate reduction rate and electron donor for each species is given. The temperatures that are highlighted indicate those experiments that were carried out at a significantly different temperature than the majority of the experiments (the majority of the experiments were carried out at 28 °C).

Microorganism	ε_S	1σ	ε_O	1σ	θ	1σ	Habitat	TYC	EQ	P^a	SRR^b	Electron donor
Desulfosarcina variabilis	22.9	3.3	5.3	0.7	0.86	0.15	Marine mud	28	28.3	C	3.7	Acetate
Desulfobulbus marinus	11.9	1.4	2.1	0.3	0.35	0.05	Marine mud	28	28.3	I	4.12	Propionate
Desulfococcus niacini	20.7	2.3	4.1	1.3	0.66	0.20	Marine mud	30	27.24	C	0.5	Acetate
Desulfocella halophila	8.5	0.4	3.8	1.5	0.67	0.34	Great Salt Lake	28	28.3	I	2.04	Pyruvate
Desulfobulbus elongates	6.8	1.7	0.6	0.4	0.10	0.06	Sewage digester	28	28.3	I	3.53	Propionate
Desulfofrigus oceanense	22.7	1.1	2.9	0.2	0.36	0.03	Arctic Marine Mud	9	32.07	C	10.4	Acetate
Desulfobacca acetoxidans	28.6	4.1	4.8	0.9	1.13	0.28	Anaerobic sludge	37	25.84	C	2.43	Acetate
Desulfotomaculum geothermicum	15	2.6	1.4	1	0.20	0.15	Deep aquifer	50	23.8	I	4.05	Lactate
Desulfonema magnum	29.6	2.4	2.8	1.6	0.42	0.23	Marine mud	28	28.3	C	14.63	Benzoate
Desulfobacterium autotrophicum	13.4	1.3	−2.3	1.7	−0.29	0.23	Marine mud	28	28.3	C	7.75	Butyrate
Desulfonatronovirio hydrogenovorans	14.8	6.8	−0.9	1.6	−0.12	0.22	Alkaline lake mud	28	28.3	I	2.54	Formate
Desulfovibrio profundus	6.2	1.9	−0.4	0.3	−0.06	0.05	Deep-sea sediment	28	28.3	I	8.5	Lactate

See text for details. Units are 10^{-15} mol/cell/day.
[a] P is for pathway and the letter refers to complete (C)- vs. incomplete (I)-oxidizing bacteria.
[b] Calculated based on cell counts made during growth of the experiments and increase in sulfide concentration.

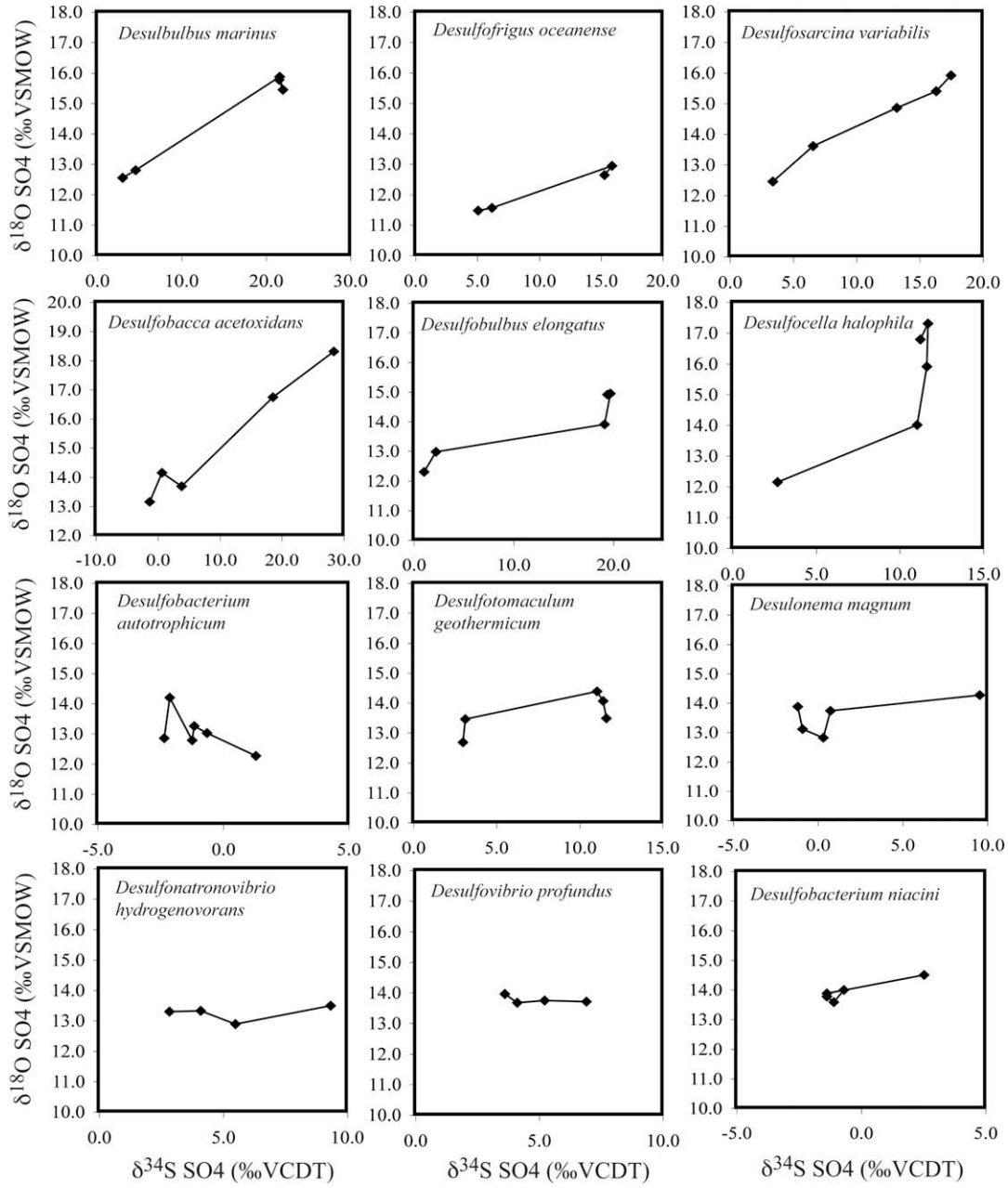

Fig. 5. Time evolution of the oxygen and sulfur isotope composition for the 12 studied strains.

Fig. 5 depicts the time evolution of $\delta^{34}S_{SO4}$ vs. $\delta^{18}O_{SO4}$ for each of the twelve strains studied. Of the twelve strains, half exhibit a positive relationship between the $\delta^{34}S_{SO4}$ and $\delta^{18}O_{SO4}$ of the evolving sulfate pool. These strains are *Desulfobulbus marinus*, *Desulfobulbus elongatus*, *Desulfosarcina variabilis*, *D. oceanense*, *Desulfobacca acetoxidans*, and *Desulfocella halophila*. Of these six strains, one shows an initial correlation between $\delta^{34}S_{SO4}$ and $\delta^{18}O_{SO4}$, but subsequently the $\delta^{18}O_{SO4}$ becomes enriched without further increase in $\delta^{34}S_{SO4}$ (*D. halophila*). The remaining six strains exhibit little, not resolvable, or even a negative enrichment in $\delta^{18}O_{SO4}$ over the growth of the bacterial culture. These strains are *Desulfovibrio profundus*, *Desulfonatronovibrio hydrogenovorans*, *Desulfobacterium niacini*, *Desulfotomaculum geothermicum*, *Desulfonema magnum*, and *Desulfobacterium autotrophicum*.

Fig. 6a and b shows plots of ε_O vs. ε_S and ε_O vs. the parameter θ_O (respectively) as calculated for growth experiments with the twelve strains. We find poor correlation between ε_S and ε_O (Fig. 6a) and between θ_O and ε_S (Fig. 6b). The experiments are divided into two groups based on complete vs. incomplete electron donor oxidation. In agreement with Detmers et al. (2001), complete-oxidizing sulfate-reducing bacteria (black squares) fractionate sulfur and oxygen isotopes more strongly than incomplete-oxidizing strains (gray squares).

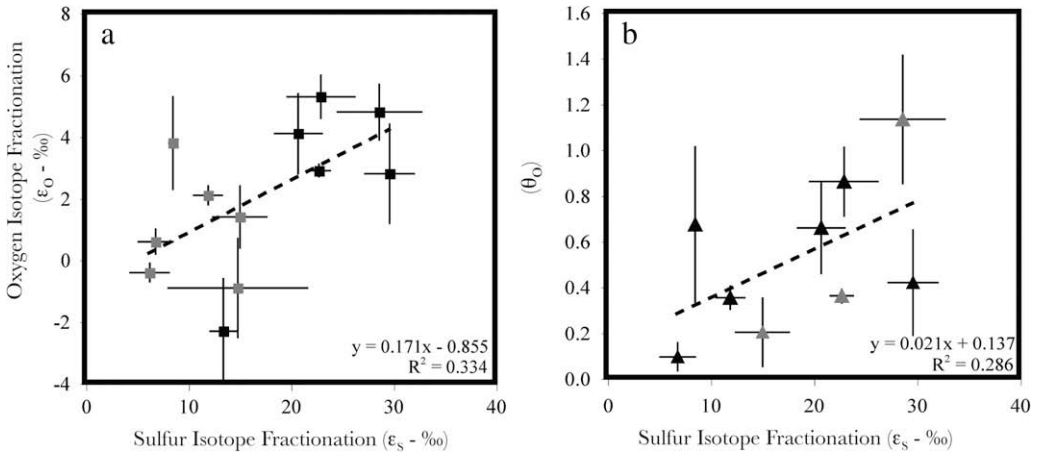

Fig. 6. Crossplots of the calculated oxygen and sulfur isotope fractionation and parameter θ_O for the various species. The error bars given represent 1σ standard deviation from calculated regression lines (Table 2). (a) Crossplot of the calculated kinetic isotope fractionation for sulfur and oxygen isotopes (ε_S vs. ε_O) determined via a Rayleigh distillation model (see text for details). The grey triangles represent incomplete-oxidizing bacteria and the black squares represent complete-oxidizing bacteria. (b) Crossplot of the calculated kinetic isotope fractionation for sulfur vs. the oxygen isotope exchange parameter (ε_S vs. θ_O). Negative values for parameter θ_O are not included in Fig. 6b because they are mathematical artifacts. Data in black are strains that were grown at 28 °C, where data in grey were grown at other temperatures and thus may have additional temperature effects on the oxygen isotope equilibration with water. All data provided in Table 2.

5. DISCUSSION

For the twelve strains of sulfate-reducing bacteria grown with identical starting $\delta^{18}O_{SO4}$ and $\delta^{18}O_{H2O}$, we find that while all strains show progressive enrichment in ^{34}S in the residual sulfate pool with growth, only half the strains exhibit enrichment in ^{18}O, while the other half show no change in oxygen isotopes. First considering the strains that show an increase in the $\delta^{18}O_{SO4}$ with progressive DSR, we recall that if APS reduction is rate-limiting in a plot of $\delta^{34}S_{SO4}$ vs. $\delta^{18}O_{SO4}$ there should be a single slope among these strains corresponding to the ratio of the kinetic sulfur and oxygen isotope effects (Eq. (1)). A composite plot of $\delta^{34}S_{SO4}$ vs. $\delta^{18}O_{SO4}$ plot is shown in Fig. 7 (the previously hypothesized 1:4 oxygen–sulfur isotope fractionation is shown as a black dashed line), where the lines in gray correspond to the strains that exhibited a positive $\delta^{34}S_{SO4}$ vs. $\delta^{18}O_{SO4}$ trend during growth. Although the slopes of these gray lines (for *D. marinus*, *D. elongates*, *D. variabilis*, *D. oceanense*, *D. acetoxidans*, and *D. halophila*) are somewhat similar, they do differ among strains, allowing us to conclude that APS reduction is likely not rate-limiting in these experiments and that a combination of kinetic and equilibrium isotope effects for oxygen isotopes is expressed. This observation is further confirmed by the poor correlation between both the calculated oxygen and sulfur isotope fractionation for all strains (ε_O and ε_S – Fig. 6a).

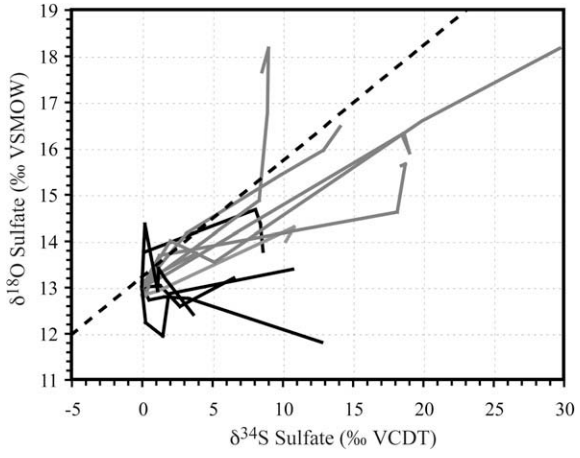

Fig. 7. A composite plot of $\delta^{34}S_{SO4}$ vs. $\delta^{18}O_{SO4}$ for all strains. The lines in gray are our the strains that show increased $\delta^{18}O_{SO4}$ with growth and the lines in black are the strains that show little or no change in $\delta^{18}O_{SO4}$ with growth. The dashed black line is the previously hypothesized 1:4 oxygen–sulfur fractionation ratio. See text for details.

The bacterial strains that exhibit little or no change in the $\delta^{18}O_{SO4}$ during growth but continual enrichment in ^{34}S may provide more information on the possible expression of a kinetic oxygen isotope effect during DSR. There are two reasons why there may be no change in the $\delta^{18}O_{SO4}$ during DSR. First, the starting $\delta^{18}O_{SO4}$ may be equal to the apparent oxygen isotope equilibrium ($\delta^{18}O_{\text{apparent equilibrium}}$), such that as the strain grows there is little change in the residual sulfate $\delta^{18}O_{SO4}$. Second, the reduction of APS to sulfite for these strains could be rate-limiting (and therefore not reversible) and the kinetic oxygen isotope effect for APS reduction ($\varepsilon^{18}O_{APS-SO3}$) could be close to zero or hidden in the analytical error of the measurements we made. We will consider each of these in turn and conclude why we think the second option is most likely.

The first hypothesis assumes that the initial oxygen isotope composition of sulfate is similar to the $\delta^{18}O_{\text{apparent equilibrium}}$, resulting in little change in the oxygen isotope composition of sulfate over the course of the experiment. Since six investigated strains exhibit an increase in the $\delta^{18}O_{SO4}$ and because the initial $\delta^{18}O_{SO4}$ was identical for all experiments (13.22‰, $n = 12$), $\delta^{18}O_{\text{apparent equilibrium}}$ for the strains that show no increase in the $\delta^{18}O_{SO4}$ would need to be lower than $\delta^{18}O_{\text{apparent equilibrium}}$ for the group that

showed an increase in the $\delta^{18}O_{SO4}$ for this hypothesis to be valid. The consequences of this condition can be explored using Eq. (2):

$$\delta^{18}O_{\text{apparent equilibrium}} = \delta^{18}O_{\text{water}} + \varepsilon^{18}O_{\text{exchange}} + (\phi_{4b}/\phi_{5b}) \times \varepsilon^{18}O_{\text{APS–SO3}}.$$

The only strain-specific parameter in Eq. (2) is the ratio ϕ_{4b}/ϕ_{5b} – the parameters $\delta^{18}O_{\text{water}}$, $\varepsilon^{18}O_{\text{exchange}}$, and $\varepsilon^{18}O_{\text{APS–SO3}}$ are the same among these bacterial strains (Table 2). Therefore, for this hypothesis to be true, the ratio ϕ_{4b}/ϕ_{5b} for the strains that show no change in the $\delta^{18}O_{SO4}$ with growth must be lower than the ratio ϕ_{4b}/ϕ_{5b} for the strains that show an increase in the $\delta^{18}O_{SO4}$ with growth. Our calculated sulfur isotope fractionation can help place constraints on the ratio ϕ_{4b}/ϕ_{5b} during the growth of these strains, because sulfur isotope fractionation larger than 25‰ requires reversibility of APS reduction ($\phi_{5b} > 0$). Consequently, the ratio ϕ_{4b}/ϕ_{5b} must be small for the strains where ε_S is larger than 25‰ (e.g., *D. magnum* and *D. acetoxidans*) and larger for the experiments where ε_S is smaller than 25‰, (e.g., *D. autotrophicum*, *D. profundus*, and *D. hydrogenoverans*). All five of these examples, however, show little or no change in the $\delta^{18}O_{SO4}$ with growth. Therefore, the ratio of ϕ_{4b}/ϕ_{5b} required for the sulfur isotope data disagrees with the ratio of ϕ_{4b}/ϕ_{5b} required for the oxygen isotope data. We conclude that this first hypothesis is unlikely, namely that $\delta^{18}O_{\text{apparent equilibrium}}$ for the strains that exhibited no change in the $\delta^{18}O_{SO4}$ with growth is lower than the $\delta^{18}O_{\text{apparent equilibrium}}$ for the remaining strains.

This leaves us with a second explanation for the strains that exhibit no change in the $\delta^{18}O_{SO4}$ with growth, that APS reduction is nearly rate-limiting ($\phi_{4b}/\phi_{5b} \to \infty$) and that $\varepsilon^{18}O_{\text{APS–SO3}}$ is close to zero or nested within the analyt-

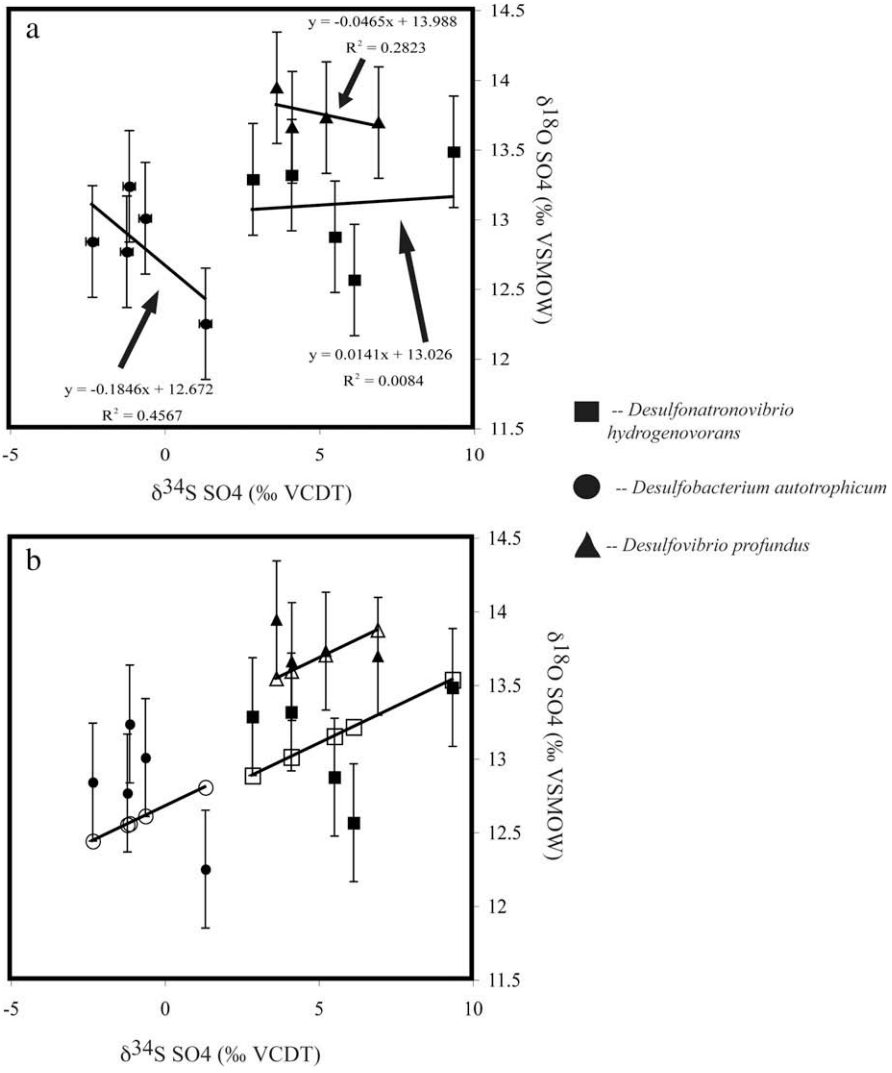

Fig. 8. $\delta^{18}O_{SO4}$ vs. $\delta^{34}S_{SO4}$ crossplots for strains with calculated negative ε_O. (a) A $\delta^{18}O_{SO4}$ vs. $\delta^{34}S_{SO4}$ crossplot of the actual measurements for *Desulfonatronovibrio hydrogenvorans* (squares), *Desulfobacterium autotrophicum* (circles), and *Desulfovibrio profundus* (triangles). Error bars for oxygen isotope measurements are 0.4‰. (b) The same data as 8a (in solid symbols) but including a hypothetical $\delta^{18}O_{SO4}$ evolution if the kinetic oxygen isotope effect (ε_O) is 2.5‰ (hollow symbols). For most data points measured, this is within the estimated error. See text for details.

ical error of our measurements. The isotopic change during the growth of three strains that show a negative correlation between $\delta^{18}O_{SO4}$ and $\delta^{34}S_{SO4}$ (*D. hydrogenovorans*, *D. autotrophicum*, and *D. profundus*) can help constrain how large a kinetic oxygen isotope effect (ε_O) could be nested within the analytical error of our measurement. When we take these three strains, we can calculate that a ε_O value as large as 2.5‰ could be hidden within the error of our data (Fig. 8b). Out of the three investigated strains, *D. hydrogenovorans* has the highest sulfur isotope fractionation with a calculated ε_S of 14.8‰. The ratio between ε_S and ε_O for this strain is 6:1 (14.8:2.5). In the scenario described in Section 2 where APS reduction is rate-limiting (as we have shown is likely the case for this strain) the ratio between ε_S and ε_O is equivalent to the ratio between $\varepsilon^{34}S_{APS-SO3}$ and $\varepsilon^{18}O_{APS-SO3}$. Using the previously published value of 25‰ for $\varepsilon^{34}S_{APS-SO3}$, the kinetic oxygen isotope effect during the reduction of APS to sulfite ($\varepsilon^{18}O_{APS-SO3}$) could consequently be as high as 4‰.

So far, we have not addressed the question if oxygen isotope exchange between water and sulfur intermediates could take place upstream of APS but have relied on our model assumption that this exchange occurs downstream of APS. Our experiments that show no change in ^{18}O but enrichment in ^{34}S, however, indicate our model assumption is valid. If the lack of change in the $\delta^{18}O_{SO4}$ was due to suppression of an oxygen isotope effect upstream of APS, the result should be suppression of the kinetic sulfur isotope effect during APS reduction, which is not observed. Thus, oxygen isotope effects (kinetic or exchange between water and sulfur intermediates) upstream of APS are likely very small.

6. OUTLOOK

Our study suggests that a kinetic oxygen isotope effect related to the reduction of APS to sulfite can be expressed when APS reduction is rate-limiting. The results from our batch culture experiments suggest the magnitude of this effect may be smaller than 4‰, much smaller than the sulfur isotope effect linked to this step (25‰). We can ask whether such a small effect is of any importance when compared to the oxygen isotope effects caused by isotope exchange with water. The significance of even a small kinetic isotope effect becomes evident when we consider the equation for $\delta^{18}O_{apparent\ equilibrium}$:

$$\begin{aligned}\delta^{18}O_{apparent\ equilibrium} &= \delta^{18}O_{water} + \varepsilon^{18}O_{exchange} \\ &\quad + (\phi_{4b}/\phi_{5b}) \times \varepsilon^{18}O_{APS-SO3} \\ &= \delta^{18}O_{water} + \varepsilon^{18}O_{exchange} \\ &\quad + (\phi_{4b}/\phi_{5b}) \times 4‰. \end{aligned} \quad (4)$$

If APS reduction is fully reversible, the ratio between APS reduction (φ_{4b}) and sulfite oxidation to APS (φ_{5b}) is one, and the impact of kinetic oxygen isotope fractionation on the apparent oxygen isotope equilibrium value would be +4‰ (Fig. 3 trend C). However, if APS reduction is not fully reversible ($\varphi_{4b}/\varphi_{5b} > 1$), the influence of the kinetic oxygen isotope effect on the apparent equilibrium would be multiplied by the ratio of these fluxes, pushing $\delta^{18}O_{apparent\ equilibrium}$ even higher (Fig. 3 trend B). This prediction can be tested in future DSR experiments with oxygen isotope compositions of starting sulfate close to the expected equilibrium.

Our plot of ε_S vs. θ_O (Fig. 6b) suggests that differences in cell membrane composition (e.g., the gram-positive *Desulfotomaculum* strain vs. all other strains, which were gram-negative) did not result in noticeable differences in oxygen isotope fractionation. Likewise, temperature differences in our study, which have the potential to produce and amplify isotope effects (Brüchert et al., 2001; Canfield et al., 2006) and that are expected to affect equilibrium isotope effects did not yield a clear pattern (Table 2 and Fig. 6b). Experiments carried out at 9 °C (*D. oceanense*) and at 50 °C (*D. geothermicum*) both fall below the regression line relative to experiments performed at 28 °C (Fig. 6b). Finally from Table 2 it is apparent that neither ε_S nor ε_O correlate in any obvious way with the cell-specific sulfate reduction rates among these diverse strains. More DSR studies are needed that address environmental parameters, such as temperature and the type of electron donor.

For most strains, the samples for isotope analysis were obtained during the lag, exponential and stationary phases. Cell-specific sulfate reduction rates decrease substantially during the stationary growth phase, possibly increasing the residence time of the intermediates with potential to exchange oxygen isotope with water. Insufficient data are available from the different growth phases to address the possibility of enhanced oxygen isotope fractionation during the stationary phase. However, the isotope trend for the strain *D. halophila* shows an initial correlation between $\delta^{34}S_{SO4}$ and $\delta^{18}O_{SO4}$, followed by isotopic enrichment in the $\delta^{18}O_{SO4}$ without further increase in $\delta^{34}S_{SO4}$ (Fig. 5). It is possible that the effect of oxygen isotope exchange increased relative to the sulfur isotope effects during the transition of this strain from the exponential to the stationary phase. These observations should be followed up with DSR experiments that allow monitoring the isotope effects during exponential and stationary growth phase.

7. CONCLUSIONS

We analyzed the relationship between oxygen and sulfur isotope compositions of sulfate during the batch culture growth of twelve strains of sulfate-reducing bacteria using a model that includes kinetic sulfur and oxygen isotope effects and oxygen isotope exchange between sulfite and water. Our data indicate that the kinetic oxygen isotope effect related to APS reduction must be less than 4‰. Although small, this isotope fractionation could impact estimates of the oxygen isotope equilibrium between sulfate and water. This impact is because the kinetic isotope effect will be multiplied by the ratio of the forward-to-backwards flux of APS to sulfite. Thus, strong reversibility of APS reduction yields less expression of the kinetic oxygen isotope effect and lower overall apparent oxygen isotope equilibrium values. For the majority of the strains studied oxygen isotope exchange between some sulfur intermediate and water is important. Thus, even when sulfur isotope fractionation is low (i.e., much smaller than 25‰), the reduction of APS to sulfite must be reversible and does

not limit the overall rate of sulfate reduction. Our findings show that paired analysis of oxygen and sulfur isotopes in sulfate yields added insight into our exploration of DSR. At the same time our results confirm that more work is needed.

ACKNOWLEDGMENTS

Financial support was provided for this project by the Miller Institute for Basic Research (A.V.T. and G.S.E.), the Canadian Institute for Advanced Research (A.V.T. and D.P.S.), NSF-OCE-0452329 (D.P.S.), the Max Planck Society (V.B. and B.B.), and the NASA Exobiology Program (T.W.L.). Reviews by AE J. Farquhar and the external reviewers greatly improved this manuscript. Discussions with Don DePaolo and Edwin Schauble improved this paper significantly.

APPENDIX A. DERIVATION OF THE EQUATION FOR OXYGEN ISOTOPE EQUILIBRIUM

1. Calculation of the isotope mass balance for APS-pool.

We first investigate the sulfur mass balance of the APS-pool by calculating the derivative after the time of the amount of sulfur, which equals the fluxes in and out of the pool (Fig. 1).

$$\frac{d}{dt}\mathrm{M_{APS}} = +\phi_{4a} - \phi_{4b} - \phi_{5a} + \phi_{5b}. \tag{A-1}$$

Correspondingly, we can also calculate the derivative after the time for the oxygen isotope composition of this pool, which equals the fluxes times their isotope composition.

$$\begin{aligned}\frac{d}{dt}\left(\mathrm{M_{APS}}\times\delta^{18}\mathrm{O_{APS}}\right) = &+\phi_{4a}\times\delta^{18}\mathrm{O_{SO4\_internal}} - \phi_{4b}\\ &\times\left(\delta^{18}\mathrm{O_{APS}} - \varepsilon^{18}\mathrm{O_{APS\text{-}SO3}}\right) - \phi_{5a}\\ &\times\delta^{18}\mathrm{O_{APS}} + \phi_{5b}\times\left(\delta^{18}\mathrm{O_{H2O}} + \varepsilon^{18}\mathrm{O_{exchange}}\right).\end{aligned} \tag{A-2}$$

Next, we use the product rule for derivations.

$$\frac{d}{dt}\left(\mathrm{M_{APS}}\times\delta^{18}\mathrm{O_{APS}}\right) = \frac{d}{dt}\mathrm{M_{APS}}\times\delta^{18}\mathrm{O_{APS}} + \mathrm{M_{APS}}\times\frac{d}{dt}\delta^{18}\mathrm{O_{APS}}. \tag{A-3}$$

We combine now Eqs. (A-1), (A-2), and (A-3).

$$\begin{aligned}&(+\phi_{4a} - \phi_{4b} - \phi_{5a} + \phi_{5b})\times\delta^{18}\mathrm{O_{APS}} + \mathrm{M_{APS}}\times\frac{d}{dt}\delta^{18}\mathrm{O_{APS}}\\ &\quad= +\phi_{4a}\times\delta^{18}\mathrm{O_{SO4\_internal}} - \phi_{4b}\times\left(\delta^{18}\mathrm{O_{APS}} - \varepsilon^{18}\mathrm{O_{APS\text{-}SO3}}\right)\\ &\qquad- \phi_{5a}\times\delta^{18}\mathrm{O_{APS}} + \phi_{5b}\times\left(\delta^{18}\mathrm{O_{H2O}} + \varepsilon^{18}\mathrm{O_{exchange}}\right).\end{aligned} \tag{A-4}$$

From this follows:

$$\begin{aligned}\mathrm{M_{APS}}\times\frac{d}{dt}\delta^{18}\mathrm{O_{APS}} = &\ \phi_{4a}\times\left(\delta^{18}\mathrm{O_{SO4\_internal}} - \delta^{18}\mathrm{O_{APS}}\right)\\ &+ \phi_{4b}\times\varepsilon^{18}\mathrm{O_{APS\text{-}SO3}} + \phi_{5b}\\ &\times\left(\delta^{18}\mathrm{O_{H2O}} + \varepsilon^{18}\mathrm{O_{exchange}} - \delta^{18}\mathrm{O_{APS}}\right).\end{aligned} \tag{A-5}$$

2. We are interested in the apparent equilibrium value. The apparent equilibrium is reached when the oxygen isotope composition of the extracellular sulfate does not change anymore. In our simplified model (Fig. 1), we assume that there are no oxygen isotope fractionations involved in the fluxes between extracellular sulfate and the APS pool. Therefore, in the model calculation for steady state conditions, the δ^{18}O of APS and the δ^{18}O of intracellular and extracellular sulfate are equal.

$$\delta^{18}\mathrm{O_{SO4\_external\_steady}} = \delta^{18}\mathrm{O_{SO4\_internal\_steady}} = \delta^{18}\mathrm{O_{APS\_steady}}.$$

The equation is simplified to:

$$\begin{aligned}\mathrm{M_{APS}}\times\frac{d}{dt}\delta^{18}\mathrm{O_{APS}} &= 0(\text{steady state assumption})\\ &= \phi_{4b}\times\varepsilon^{18}\mathrm{O_{APS\text{-}SO3}} + \phi_{5b}\\ &\quad\times\left(\delta^{18}\mathrm{O_{H2O}} + \varepsilon^{18}\mathrm{O_{exchange}}\right.\\ &\quad\left.- \delta^{18}\mathrm{O_{SO4\_external\_steady}}\right)\\ &\Rightarrow \delta^{18}\mathrm{O_{SO4\_external\_steady}}\\ &= \delta^{18}\mathrm{O_{H2O}} + \varepsilon^{18}\mathrm{O_{exchange}}\\ &\quad+\frac{\phi_{4b}}{\phi_{5b}}\times\varepsilon^{18}\mathrm{O_{APS\text{-}SO3}}.\end{aligned} \tag{A-6}$$

REFERENCES

Aharon P. and Fu B. (2000) Microbial sulfate reduction rates and sulfur and oxygen isotope fractionations at oil and gas seeps in deepwater Gulf of Mexico. *Geochim. Cosmochim. Acta* **64**(2), 233–246.

Basharmal M. (1985) *The Isotopic Composition of Sulphur Compounds in Landfills*. MSc thesis, U. Waterloo, Waterloo, Ont, Canada.

Betts R. H. and Voss R. H. (1970) The kinetics of oxygen exchange between the sulfite ion and water. *Can. J. Chem.* **48**, 2035–2041.

Böttcher M. E., Oelschläger B., Höpner T., Brumsack H. J. and Rullkötter J. (1998) Sulfate reduction related to the early diagenetic degradation of organic matter and "black spot" formation in tidal sandflats of the German Wadden Sea (southern North Sea): stable isotope (C-13, S-34, O-18) and other geochemical results. *Org. Geochem.* **29**, 1517–1530.

Böttcher M. E., Bernasconi S. M. and Brumsack H.-J. (1999) Carbon, sulfur, and oxygen isotope geochemistry of interstitial waters from the western Mediterranean. In *Proceedings of the Ocean Drilling Program, Scientific Results*, vol. 161 (eds. R. Zahn, M. C. Comas and A. Klaus), pp. 413–421. Proceedings of the Ocean Drilling Program, Scientific Results. Ocean Drilling Program, College Station, TX.

Böttcher M., Thamdrup B. and Vennemann T. W. (2001) Oxygen and sulfur isotope fractionation during anaerobic bacterial disproportionation of sulfur. *Geochim. Cosmochim. Acta* **60**, 1601–1609.

Böttcher M., Thamdrup B., Gehre M. and Theune A. (2005) 34S/32S and 18O/16O fractionation during sulfur disproportionation by *Desulfobulbus propionicus*. *Geomicrobiol. J.* **22**, 219–226.

Bottrell S. H., Parkes R. J., Cragg B. A. and Raiswell R. (2000) Isotopic evidence for anoxic pyrite oxidation and stimulation of bacterial sulphate reduction in marine sediments. *J. Geol. Soc.* **157**, 711–714.

Brüchert V., Knoblauch C. and Jørgensen B. B. (2001) Microbial controls on the stable sulfur isotopic fractionation during bacterial sulfate reduction in Arctic sediments. *Geochim. Cosmochim. Acta* **65**, 753–766.

Brüchert V. (2004) Physiological and ecological aspects of sulfur isotope fractionation during bacterial sulfate reduction. In

Sulfur Biogeochemistry – Past and Present, vol. 379 (eds. J. P. Amend, K. J. Edwards and T. W. Lyons), pp. 1–16. Geological Society of America Special Paper. Geological Society of America, Boulder CO, USA.

Brunner B. and Bernasconi S. M. (2005) A revised isotope fractionation model for dissimilatory sulfate reducing in sulfate reducing bacteria. *Geochim. Cosmochim. Acta* **69**, 4759–4771.

Brunner B., Bernasconi S. M., Kleikemper J. and Schroth M. J. (2005) A model for oxygen and sulfur isotope fractionation in sulfate during bacterial sulfate reduction processes. *Geochim. Cosmochim. Acta* **69**, 4773–4785.

Brunner B., Mielke R. E., Coleman M. (2006) Abiotic oxygen isotope equilibrium fractionation between sulfite and water. American Geophysical Union, Fall Meeting 2006, Eos Trans AGU 87, abstract No. V11C-0601.

Cameron E. M. (1982) Sulfate and sulfate reduction in Early Precambrian Oceans. *Nature* **296**, 145–148.

Canfield D. E. (1998) A new model for Proterozoic ocean chemistry. *Nature* **396**, 435–450.

Canfield D. E. and Teske A. (1996) Late Proterozoic rise in atmospheric oxygen concentration inferred from phylogenetic and sulphur-isotope studies. *Nature* **382**, 127–132.

Canfield D. E. (2001a) Isotope fractionation by natural populations of sulfate-reducing bacteria. *Geochim. Cosmochim. Acta* **65**, 1117–1124.

Canfield D. E. (2001b) Biochemistry of sulfur isotopes. In Stable Isotope Geochemistry: Reviews in Mineralogy and Geochemistry, vol. 43 (eds. J.W. Valley and D. Cole), pp. 607-636.

Canfield D. E. (2004) The evolution of the Earth surface sulfur reservoir. *Am. J. Sci* **304**, 839–861.

Canfield D. E., Olesen C. A. and Cox R. P. (2006) Temperature and its control of isotope fractionation by a sulfate-reducing bacterium. *Geochim. Cosmochim. Acta* **70**, 548–561.

Detmers J., Brüchert V., Habicht K. S. and Kuever J. (2001) Diversity of sulfur isotope fractionations by sulfate-reducing prokaryotes. *Appl. Environ. Microbiol.* **67**, 888–894.

Farquhar J., Johnston D. T., Wing B. A., Habicht K. S., Canfield D. E., Airieau S. and Thiemens M. H. (2003) Multiple sulphur isotopic interpretations of biosynthetic pathways: implications for biological signatures in the sulphur isotope record. *Geobiology* **1**, 27–36.

Farquhar J., Canfield D. E., Masterson A., Bao H. and Johnston D. T. (2008) Sulfur and oxygen isotope study of sulfate reduction in experiments with natural populations from Faellestrand, Denmark. *Geochim. Cosmochim. Acta* **72**, 2805–2821.

Fritz P., Basharmal G. M., Drimmie R. J., Ibsen J. and Qureshi R. M. (1989) Oxygen isotope exchange between sulfate and water during bacterial reduction of sulfate. *Chem. Geol.* **79**, 99–105.

Fritz G., Büchert T. and Kroneck P. M. H. (2002) The function of the (4Fe–4S) clusters and FAD in bacterial and archaeal adenylylsulfate reductases. *J. Biol. Chem.* **277**, 26066–26073.

Grinenko V. A. and Ustinov V. I. (1990) Dynamics of sulfur and oxygen isotope fractionation during bacterial sulfate reduction. *Geokhimiya* **9**, 1241–1251.

Habicht K. S. and Canfield D. E. (2001) Isotope fractionation by sulfate-reducing natural populations and the isotopic composition of sulfide in marine sediments. *Geology* **29**, 555–558.

Habicht K. S., Gade M., Thamdrup B., Berg P. and Canfield D. E. (2002) Calibration of sulfate levels in the Archaean ocean. *Science* **298**, 2372–2374.

Holser W. T. and Kaplan I. R. (1966) Isotope geochemistry of sedimentary sulfates. *Chem. Geol.* **1**, 93–135.

Horner D. A. and Connick R. E. (2003) Kinetics of oxygen exchange between the two isomers of bisulfite ion, disulfite ion ($S_2O_5^{2-}$), and water as studied by oxygen-17 Nuclear Magnetic Resonance Spectroscopy. *Inorg. Chem.* **42**, 1884–1894.

Jørgensen B. B. (1979) A theoretical model of the sulfur isotope distribution in marine sediments. *Geochim. Cosmochim. Acta* **43**, 363–374.

Jørgensen B. B. (1990) A thiosulfate shunt in the sulfur cycle of marine sediments. *Science* **249**, 152–154.

Johnston D. T., Wing B. A., Farquhar J., Kaufman A. J., Strauss H., Lyons T. W., Kah L. C. and Canfield D. E. (2005) Active microbial sulfur disproportionation in the Mesoproterozoic. *Science* **310**, 1477–1479.

Kaplan I. R. and Rittenberg S. C. (1964) Microbiological fractionation of sulphur isotopes. *J. Gen. Microbiol.* **34**, 195–202.

Kah L. C., Lyons T. W. and Frank T. D. (2004) Low marine sulphate and protracted oxygenation of the Proterozoic biosphere. *Nature* **431**, 834–838.

Kemp A. L. W. and Thode H. G. (1968) The mechanism of the bacterial reduction of sulphate and of sulphite from isotope fractionation studies. *Geochim. Cosmochim. Acta* **32**, 71–91.

Kohl I. E. and Bao H. (2006) Does enzyme-catalyzed formation of sulfate complexes cause oxygen isotope exchange during dissimilatory microbial sulfate reduction? Eos Trans AGU 87, V11C-0599.

Lloyd R. M. (1968) Oxygen isotope behavior in sulfate–water system. *J. Geophys. Res.* **73**, 6099–6110.

Mangalo M., Meckenstock R. U., Stichler W. and Einsiedl F. (2007) Stable isotope fractionation during bacterial sulfate reduction is controlled by reoxidation of intermediates. *Geochim. Cosmochim. Acta* **71**, 4161–4171.

Mandernack K., Krouse H. R. and Skei J. M. (2003) A stable sulfur and oxygen isotopic investigation of sulfur cycling in an anoxic marine basin, Framvaren Fjord, Norway. *Chem. Geol.* **195**, 181–200.

McKenzie W. F. and Truesdell A. H. (1977) Geothermal reservoir temperatures estimated from the oxygen isotope compositions of dissolved sulfate and water from hot springs and shallow drillholes. *Geothermics* **5**, 51–61.

Mitzutani Y. and Rafter T. A. (1969) Oxygen isotope composition of sulphates: 3. Oxygen isotope fractionation in the bisulphate ion–water system. *NZ J. Sci.* **12**, 54–59.

Mizutani Y. and Ragter T. A. (1969) Oxygen Isotopic composition of sulphates 5. Isotopic composition of sulphate in rain water Gracefield, New Zealand. *NZ J. Sci.* **12**, 69–75.

Mizutani Y. and Rafter T. A. (1973) Isotopic behaviour of sulphate oxygen in the bacterial reduction of sulphate. *Geochem. J.* **6**, 183–191.

Mizutani Y. (1972) Isotopic composition and underground temperature of the Otake geothermal water, Kyushu, Japan. *Geochem. J.* **6**, 67–73.

Paytan A., Kastner M., Campbell D. and Thiemens M. H. (2004) Seawater sulfur isotope fluctuations in the Cretaceous. *Science* **304**, 1663–1665.

Peck H. D. and Stulberg M. P. (1962) O18 studies on the mechanism of sulfate formation and phosphorylation in extracts of *Thiobacillus thioparus*. *J. Biol. Chem.* **237**(5), 1648–1652.

Rees C. E. (1973) A steady-state model for sulphur isotope fractionation in bacterial reduction processes. *Geochim. Cosmochim. Acta* **37**, 1141–1162.

Rudnicki M. D., Elderfield H. and Spiro B. (2001) Fractionation of sulfur isotopes during bacterial sulfate reduction in deep ocean sediments at elevated temperatures. *Geochim. Cosmochim. Acta* **65**, 777–789.

Turchyn A. V. and Schrag D. P. (2006) Cenozoic evolution of the sulfur cycle: insight from oxygen isotopes in marine sulfate. *Earth Planet. Sci. Lett.* **241**, 763–779.

Van Stempvoort D. R. and Krouse H. R. (1994) Controls of $\delta^{18}O$ in sulfate; review of experimental data and application to specific environments. In *Environmental Geochemistry of Sulfide Oxidation*. American Chemical Society, pp. 446–480.

Wadham J. L., Bottrell S., Tranter M. and Raiswell R. (2004) Stable isotope evidence for microbial sulphate reduction at the bed of a polythermal high Arctic glacier. *Earth Planet. Sci. Lett.* **219**, 341–355.

Wortmann U. G., Bernasconi S. M. and Bottcher M. E. (2001) Hypersulfidic deep biosphere indicates extreme sulfur isotope fractionation during single-step microbial sulfate reduction. *Geology* **29**, 647–650.

Wortmann U. G. and Chernyavsky B. (2007) Effect of evaporite deposition on early Cretaceous carbon and sulphur cycling. *Nature* **446**, 654–656.

Wortmann U. G., Chernyavsky B., Bernasconi S. M., Brunner B., Böttcher M. E. and Swart P. K. (2007) Oxygen isotope biogeochemistry of pore water sulfate in the deep biosphere: dominance of isotope exchange reactions with ambient water during microbial sulfate reduction (ODP Site 1130). *Geochim. Cosmochim. Acta* **71**, 4221–4232.

Zak I., Sakai H. and Kaplan I. R. (1980) Factors controlling the 18O/16O and 34S/32S isotope ratios of ocean sulfates, evaporites and interstitial sulfates from modern deep sea sediments. In *Isotope Marine Chemistry*. Institute of Geophysics and Planetary Physics, University of California Los Angeles, California 90024, USA, pp. 339–373 (Chapter 17).

Associate editor: James Farquhar